Crystallization of TiO_2 polymorphs from RF-sputtered, amorphous thin-film precursors

Cite as: AIP Advances 10, 025109 (2020); doi: 10.1063/1.5140368
Submitted: 26 November 2019 • Accepted: 23 January 2020 •
Published Online: 6 February 2020

O. Agirseven,[1] D. T. Rivella, Jr.,[1] J. E. S. Haggerty,[1] P. O. Berry,[1] K. Diffendaffer,[1] A. Patterson,[1] J. Kreb,[1] J. S. Mangum,[2] B. P. Gorman,[2] J. D. Perkins,[3,a)] B. R. Chen,[4] L. T. Schelhas,[4] and J. Tate[1,b)]

AFFILIATIONS

[1]Department of Physics, Oregon State University, Corvallis, Oregon 97331, USA
[2]Department of Metallurgical and Materials Engineering, Colorado School of Mines, Golden, Colorado 80401, USA
[3]National Renewable Energy Laboratory, Golden, Colorado 80401, USA
[4]SLAC National Accelerator Laboratory, Menlo Park, California 94025, USA

[a)]**Current address:** Applied Chemicals and Materials Division, NIST, Boulder, Colorado 80305, USA.
[b)]**Author to whom correspondence should be addressed:** tate@physics.oregonstate.edu

ABSTRACT

Crystalline TiO_2 films of anatase, brookite, and rutile are reproducibly made from amorphous precursors deposited by RF magnetron sputtering, producing large-area, single phase films of uniform thickness. Sputtered amorphous TiO_2 precursor thin films follow the general behavior observed for amorphous precursor thin films generated by pulsed laser deposition, namely, that oxygen deficiency is necessary for the formation of brookite and rutile. We quantify the oxygen deficiency and correlate it with the long wavelength optical absorption. We find that the precursor deposition rate is also a contributing factor to phase selection and that brookite and rutile form from films deposited more rapidly and anatase from films deposited more slowly. Sputtered and pulsed laser deposited amorphous precursor films prepared with similar oxygen deficiency and similar thickness result in the same final state after annealing, but the rate for sputtered precursors is slower.

INTRODUCTION

TiO_2 is a multifunctional transparent semiconductor used in industrial and technological applications such as solar cells, sensors, lithium-ion batteries, ultra-thin capacitors, photovoltaics, photocatalysts, optical waveguides, and filters.[1–5] It has a high refractive index, a high dielectric constant, and a wide bandgap. It is stable, non-toxic, and relatively inexpensive to produce. The photocatalytic properties of TiO_2 are useful in environmental applications such as degradation of toxic wastes and removing polluting agents from air and water, as well as self-cleaning and antibacterial protective coatings.[1–3] TiO_2 has several polymorphs: rutile is the lowest energy state, while anatase and brookite are both metastable. Density functional calculations suggest that the low-energy (210) surface of TiO_2 brookite may be a better photocatalyst than the low-energy TiO_2 anatase (101) surface.[6] It is therefore useful to understand whether and how a metastable polymorph can be stabilized. Such knowledge on the TiO_2 system could be transferred to other polymorphic material systems.

We previously found that amorphous TiO_2 films grown by pulsed laser deposition (PLD) annealed to different polymorphs of crystalline TiO_2 and that the major factors determining which polymorphs formed were the pressure of oxygen during deposition and the thickness of the precursor film.[7,8] In those studies, we did not directly investigate the effect of deposition rate of the precursor films. We were also unable to say whether the results were unique to pulsed laser deposition or whether they were transferable to other deposition methods. In this study, we address those questions with the results of a similar investigation of sputter-deposited TiO_2 amorphous precursor films, which are of uniform thickness over a large area sputtered at different rates and to different thicknesses. We also present some optical and electrical properties of these TiO_2

films that illustrate the importance of the oxygen deficiency in the precursor and crystallized films.

EXPERIMENT

Precursor films are sputtered in an Orion 5 sputter deposition chamber with base pressure $<5 \times 10^{-7}$ mTorr. The target is 5-cm diameter metallic Ti (99.995%, AJA International), and the sputter gases are Ar (99.999%, Airgas) and an Ar/O_2 mix (99.998%, Airgas) at a total pressure of 2.5 mTorr. The O_2 contributes from 0.01 to 0.5 mTorr. The RF sputter power is 90 W or 100 W. The deposition rate is ~2 nm/min at 100 W and 2.5 mTorr total pressure with 2.87% O_2 and decreases with decreasing sputter power or increasing oxygen partial pressure. System limitations prevent oxygen partial pressures greater than about 5%.

The substrate is pure fused SiO_2 (GM Associates 7525-01, 99.99% with the major impurity Al at <19 ppm) typically 2.5 cm × 2.5 cm × 1 mm thick, held at ambient temperature and 10 cm from the target. The substrates are rotated at 50 rpm during deposition. The SiO_2 sample is large and uniform enough that 16 subsamples can be cut from the same film for different analyses and we are confident that all subsamples represent the same conditions. This uniformity is a significant advantage of the sputter method.

The precursor films are annealed in an AET Thermal RX Series Rapid Thermal Processing system in flowing N_2 at 10 l/s. The annealing protocol is to ramp the temperature to 400 °C in ~10 min, hold for 3–10 min, and turn off the heat so that the films cool to room temperature in about 5 min (similar to Ref. 7). The nitrogen gas is derived from boiling a liquid source that is >99.9997% pure, but the annealing oven is not hermetically sealed so that some oxygen from the ambient is surely present during the anneal. For this reason, we performed EPMA (electron probe microanalysis) to determine the change in oxygen content after annealing. We also varied the anneal procedures in a few cases to test the effect of rate (20–150 °C/min) and final temperature (320–450 °C).

Stoichiometry is determined by EPMA on films deposited simultaneously on a 1 cm × 1 cm Si substrate and annealed side-by-side in the case of crystalline films. The Si substrate avoids interference from substrate oxygen. EPMA also yields thickness if the density is known. More routinely, thickness is determined by ellipsometry in the 400–1000 nm range on a J. A. Woollam M-2000 spectroscopic ellipsometer. Further information about EPMA is given in the supplementary material.

Optical microscopy, coupled with Raman spectroscopy, establishes which phases are present. The three polymorphs and the amorphous phase have slightly different refractive indices in the visible range,[9] which renders the different phases distinguishable in an optical image. Morphology differences also aid polymorph differentiation. With experience, the polymorph identification by difference in refractive index becomes very reliable, but we always confirm the phases with Raman spectroscopy, which yields quite distinct spectra for the three polymorphs, at several points on any sample. The optical images and Raman spectra are acquired in a Horiba Jobin-Yvon LabRam 800 Raman spectrometer equipped with the LabSpec 6.0 software suite. We can distinguish features as small as 1 μm in Raman spectroscopy.

X-ray diffraction for further phase identification is performed at the Stanford Synchrotron Radiation Lightsource (SSRL) Beamline 11-3 with an x-ray wavelength of 0.9744 Å. The 2D wide-angle x-ray scattering (WAXS) patterns are collected using a Rayonix 225 detector in grazing incidence geometry. The x-ray incidence angle is 1° during the measurements to reduce the amorphous scattering from the SiO_2 substrate. Further information about the WAXS measurements is given in the supplementary material.

Optical transmission and reflection spectra are obtained in a grating spectrometer with a Xe source and Si detector in the range 250–1000 nm, with 1 nm resolution. Thin-film interference fringes complicate the interpretation of absorption, so they are removed by calculating the reflection- and interference-corrected transmission, which is $T/(1-R) \approx \exp(-\alpha d)$ in the limit of small absorption (T and R are the transmission and reflection, respectively, of the film/substrate stack, α is the absorption coefficient of the film, and d is its thickness). More details about this procedure are given in the supplementary material.

The electrical resistivity of amorphous precursor and crystalline films is measured in a Lakeshore Hall Measurement system in the van der Pauw geometry with small, Ohmic indium contacts symmetrically placed on square samples. The sample is in a liquid nitrogen dewar during measurement, and slow evaporation of the liquid keeps the temperature constant to within 1 K of a particular value for a single measurement but allows the temperature to change from 77 K to 275 K over successive measurements.

RESULTS

Oxygen content and thickness

EPMA in Table I reveals that all the precursor films are substoichiometric TiO_{2-x}. The error in the O/Ti ratio is approximately 1%–2%. Larger oxygen deficiency correlates with lower partial pressure of oxygen during deposition, as expected. After being annealed, the film oxygen content increases, indicating that some oxygen vacancies are filled. Although the anneal is under nitrogen to try to preserve the substoichiometry, a small amount of oxygen may enter the flow system from the ambient. The increase in the O/Ti ratio is of order 3%–10% and depends on the initial deficiency. The density of phase-pure films prepared on SiO_2 substrates and their corresponding precursor films is obtained by x-ray reflectivity, and these values are used to convert the EPMA areal densities to the "epma" thicknesses displayed in Table I. The thicknesses are within about 5%–15% of those obtained by ellipsometry. The crystallized films increase in density. Not all precursor films displayed in Table I resulted in brookite, rutile, or anatase, or mixtures upon annealing. In particular, the highly oxygen-deficient samples 09 and 10 did not yield interpretable Raman spectra, so we do not know the phase. However, the study quantified the oxygen stoichiometry and characterized the process as intended.

Phase identification

Figure 1 shows an optical image of an annealed TiO_2 film with three phases visible, along with the Raman spectrum corresponding to each polymorph at the locations indicated. The reference peaks are from the RRUFF Project database.[10] This film is atypical in that it has all three polymorphs, but it illustrates some common morphologies: rutile tends to grow in circular disks (unless it nucleates on a surface imperfection), while brookite and anatase are more

TABLE I. EPMA-determined stoichiometry of precursor and post-annealed TiO_{2-x} thin films deposited by RF magnetron sputtering at 100 W at various partial pressures of oxygen (pO_2). The phase analysis is quoted as a percentage of rutile (R), brookite (B), and anatase (A). An asterisk means the Raman signal is very weak. Thicknesses are determined by ellipsometry and from the EPMA analysis combined with XRR-determined density if the phase is known (see text).

Sample	pO_2 (%)	$\left[\frac{O}{Ti}\right]_{pre}$	$\left[\frac{O}{Ti}\right]_{post}$	$t_{pre,epma}$ (nm)	$t_{post,epma}$ (nm)	$t_{pre,ellip}$ (nm)	$t_{post,ellip}$ (nm)	*Phase*
09	0.43	1.11	1.21	...	...	37	48	...
10	0.43	0.78	0.88	...	...	70	72	...
32	1.18	1.66	1.79	45	47	40	43	100R
31	2.86	1.89	1.97	18	19	22	20	92B, 8R
22	2.86	1.92	1.99	20	20	24	23	B*
12	2.86	1.88	1.98	28	29	31	32	B*
30	2.86	1.82	1.87	62	60	59	61	78R, 22B
33	5.00	1.81	1.95	3.6	6.1	5.3	5.8	A*

irregular. The details of morphology and growth can be intricate and interesting, but that topic is complex and beyond the scope of this paper. For the purposes of this report, it suffices to demonstrate that we can identify the polymorphs and phase fractions easily.

Further confirmation of the phase identity by WAXS is shown in Fig. 2. These particular examples of x-ray scattering patterns are from a precursor film and its post-annealed counterpart. The precursor is x-ray amorphous, which is consistent with the Raman experiments that show no discernable Raman peaks. The diffraction pattern of this post-annealed film is consistent with a polycrystalline brookite phase of TiO_2, which is characterized by the (210) and (111) peaks around $Q = 1.78$ Å^{-1}, the distinctive (211) peak at $Q = 2.15$ Å^{-1} that has no close counterparts in rutile or anatase, and several minor peaks at larger Q that are also evident. This result agrees with the Raman spectrum, which only shows Raman peaks from brookite. From the combined X-ray diffraction, optical analysis of the phase fraction, and Raman spectroscopy, we conclude that this is cm-scale, polycrystalline brookite film with <1% of rutile. The procedure is robust and has been reproduced many times.

We see that the phases formed in the subset of films displayed in Table I qualitatively conform to the pattern observed for PLD-deposited films:[7,8] Brookite forms upon annealing precursor films deposited at intermediate oxygen pressures and thicknesses, yielding to rutile for lower pressures (cf. samples 31 and 32) and higher thicknesses (cf. samples 32 and 30). Our previous observation was that anatase results from thinner precursors prepared at higher oxygen pressure. We do indeed observe anatase at the thinner margins of samples 31 and 30, but sample 33 (expected to be anatase) at <6 nm is so thin as to yield an extremely weak Raman spectrum. Samples 22 and 12 yield homogeneous optical micrographs, but the Raman spectra are inexplicably weak but suggestive of brookite. Where the Raman signal is weak, we denote the phase with an asterisk.

Deposition rate

Figure 3 is a phase plot of 35 films of different thicknesses up to about 150 nm deposited at ambient temperature by RF magnetron sputtering at 2.8% O_2 in Ar and subsequently annealed at 400 °C. The phase fractions are determined by optical analysis of the entire film, with confirmation by Raman analysis in several areas of the film. The deposition rates differ because the sputter power changes from 100 W (near 2 nm/min) to 90 W (near 1.5 nm/min), with more subtle rate variations that result from process details. Precursor films that are deposited more slowly result in the anatase polymorph, regardless of thickness, while those deposited faster result in brookite and rutile. Within the brookite and rutile films, there is a strong tendency for brookite to form thinner films, while rutile tends to form when the precursors are thicker. We also do not

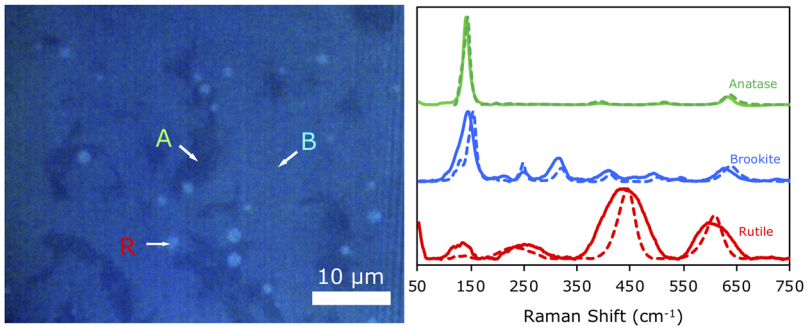

FIG. 1. Optical image of a 33-nm post-annealed film, illustrating morphology. The small, bright circular areas are rutile, the lighter irregular areas are brookite, and the darker areas are anatase. Most films are more homogeneous. The Raman spectra (solid) to the right are of the areas indicated by the arrows. The dashed lines are reference spectra from the RRUFF database (brookite R050591, anatase R070582, and rutile R060493).

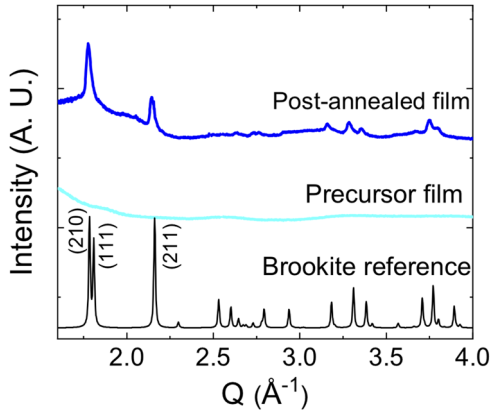

FIG. 2. WAXS patterns (intensity on a linear scale) of TiO_2 thin films deposited on SiO_2 by RF magnetron sputtering at 2.8% O_2 in Ar. The as-deposited precursor film is amorphous (light blue trace). After annealing, the thin film transformed into brookite (dark blue trace), which is consistent with the brookite reference (ICSD No. 36408, black trace). The post-annealed film is 26 nm thick and contains >99% brookite, as analyzed by Raman spectroscopy.

present detailed results, but we note that, in general, the annealing procedure is less important to the outcome of the anneal than the preparation of the precursor. In particular, ramp rate and maximum temperature do not seem to affect the end products—only the time to crystallization changes.

Optical absorption

Figure 4 is a plot of $T/(1 - R)$ as a function of wavelength,[11] the reflection (R)- and interference-corrected transmission (T) of precursor and post-annealed TiO_2 films on SiO_2 substrates. Details about the procedure are provided in the supplementary material.

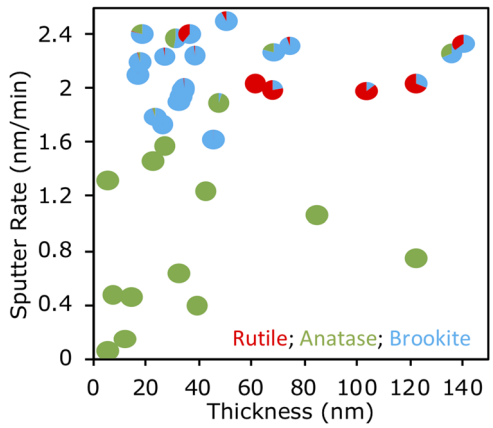

FIG. 3. Phase plot of 35 films deposited at ambient temperature by RF magnetron sputtering at 2.8% O_2 in Ar and subsequently annealed at 400 °C. Each "pie" symbol corresponds to one film, and the proportions of anatase (green), brookite (blue), and rutile (red) are indicated. Anatase tends to form from precursor films deposited at lower deposition rates for all thicknesses, and brookite and rutile result from precursor films deposited at higher deposition rates.

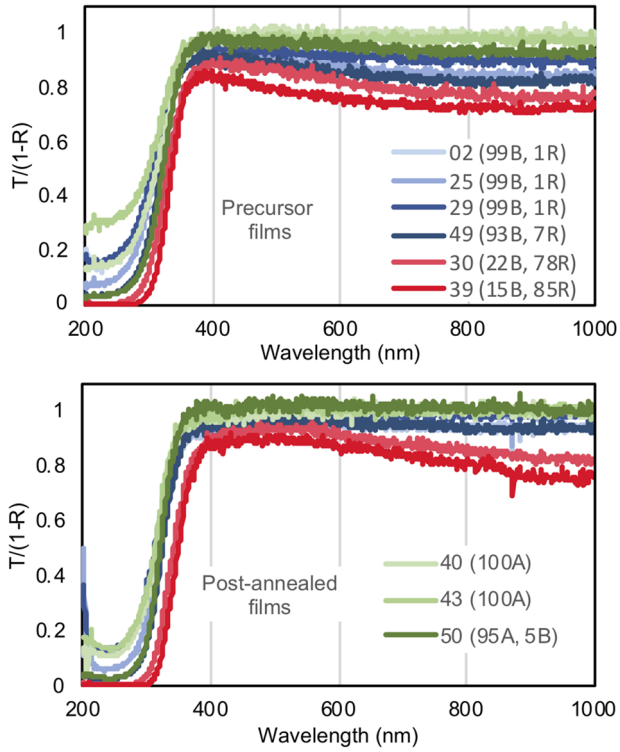

FIG. 4. Reflection-corrected and interference-corrected transmission $T/(1 - R)$ of precursor (amorphous) and corresponding post-annealed (crystalline) TiO_2 thin films deposited by RF magnetron sputtering. The films are color-coded by the polymorph that results *after* the anneal: green for anatase, red for rutile, and blue for brookite. Brookite and rutile legends appear in the upper graph and anatase legends in the lower graph to prevent overcrowding. The films are identified by number and (95A, 5B) means the film is 95% anatase and 5% brookite, for example.

The extent to which $T/(1 - R)$ deviates from unity indicates large absorption in the film. The films are color-coded by the polymorph that results *after* the anneal: green for anatase, red for rutile, and blue for brookite. The pre-anatase amorphous precursors are optically distinct from pre-brookite and pre-rutile amorphous precursors in that they have a very low absorption coefficient ($<1 \times 10^4$ cm^{-1}) across the visible and near infrared spectrum (400–1000 nm). The pre-brookite and pre-rutile amorphous precursors exhibit significantly higher absorption coefficients, which approach $3–5 \times 10^4$ cm^{-1} at the longer wavelength end. This absorption is characteristic of oxygen vacancies,[12] which fits the picture of oxygen deficient precursors producing brookite and rutile.[8] Upon annealing, the long wavelength absorption is reduced in all samples, consistent with oxygen uptake, but there is still considerable oxygen deficiency in the brookite and especially the rutile films. The strong absorption onset toward shorter wavelengths is indicative of the optical bandgap of the films. The precursors all have similar absorption onsets near 375 nm (3.3 eV) although the absorption increases more sharply for the thicker films, which in this case happens to be rutile (70–100 nm vs 30–50 for anatase and brookite). In the post-annealed films, the absorption onset moves to longer wavelengths

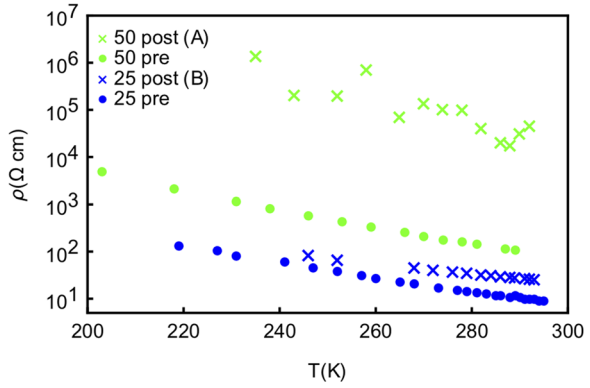

FIG. 5. Temperature-dependent resistivity of precursor (circles) and post-annealed (crosses) TiO_2 thin films deposited by RF magnetron sputtering. Sample No. 25 (blue symbols) is 99% brookite (B) and 1% rutile, and sample No. 50 is 95% anatase (A) and 5% brookite.

(3.1 eV) in the rutile films, while remaining near 3.3 eV for the anatase and brookite films. Brookite is widely reported to have the smallest bandgap of the three polymorphs, and our result is consistent. No clear difference in bandgap between anatase and brookite is found.

In Fig. 5, the temperature-dependent resistivity of two of the films from Fig. 4 is presented. The pre-anatase film is more resistive than the pre-brookite film, as expected if the oxygen deficiency contributes carriers via oxygen vacancies and/or titanium interstitials.[13] In these two cases, the resistivity of the annealed crystalline film is also larger than that of its precursor film, again consistent with a decrease in carrier density as oxygen is taken up. However, the resistivity sometimes decreases upon annealing, perhaps because the mobility increases in the crystalline phase. In general, we observe that a variable-range hopping resistivity model $\rho(T) = \rho_\infty \exp(U/k_B T)^{1/4}$ fits the amorphous precursor films better and over a larger temperature range. A thermally activated band transport model $\rho(T) = \rho_\infty \exp(E_A/k_B T)$ fits the crystalline films better, with activation energies $E_{A,\text{brookite}} \approx 150$ meV and $E_{A,\text{anatase}} \approx 350$ meV for the particular samples shown in Fig. 5. The Hall voltage is characteristic of n-type carriers as expected for oxygen vacancies in crystalline TiO_2. The carrier concentrations and mobilities at 295 K are given in Table II.

TABLE II. Carrier density (n) and mobility (μ) at 295 K of precursor and post-annealed TiO_{2-x} thin films in Fig. 5, with other relevant film properties. The phase analysis is quoted as a percentage of rutile (R), brookite (B), and anatase (A).

Sample	pO_2 (%)	n (cm^{-3})	Carrier type	$\mu\left(\frac{cm^2}{V\,s}\right)$	t (nm)	Phase
25 (pre)	2.86	1×10^{19}	N	0.05	33	Amorphous
25 (post)		7×10^{16}	N	3	36	99B, 1R
50 (pre)	2.86	7×10^{15}	N	7	51	Amorphous
50 (post)		3×10^{12}	N	45	45	95A, 5B

DISCUSSION

PLD vs sputtered precursor films

These results demonstrate that the method of annealing carefully prepared amorphous precursor films to achieve particular TiO_2 polymorphs, especially brookite, is generalizable from pulsed-laser-deposited precursor films to sputtered precursor films. Sputtering is a widely used deposition method in industrial production, whereas PLD is largely confined to research laboratories. Both are non-equilibrium deposition techniques, which are necessary to stabilize a metastable phase. The similarities are (i) that the brookite or rutile polymorphs result from annealing the more oxygen-deficient precursors, while the anatase polymorph results from annealing the less oxygen-deficient precursors and (ii) that at a particular pressure of oxygen, thinner films tend to be anatase, thicker films are brookite, and the thickest are rutile with multiple phases in the "border" regions. The specific parameters are slightly different, however. For example, we found that PLD precursors deposited at 2.5 mTorr pO_2 (also total pressure) produced high fraction brookite films in the range 65–75 nm, while sputtered precursors deposited at 0.0715 mTorr pO_2 (2.5 mTorr total pressure) produced the same brookite fraction in the range 30–45 nm. We also observed that while 400 °C appeared to be a good temperature for crystallization in both systems, films of similar thickness needed about 30% more time to crystallize in the case of sputtered precursor films. This observation suggests that the energetics of the evaporants produced by the sputter cloud and PLD plume may be different and are also important. Finally, sputtered precursors produce very uniform thickness films, whereas PLD-deposited films are non-uniform because the plume is strongly directional. The sputtered precursors have therefore yielded several-cm scale films of brookite that have <1% rutile or anatase.

Rate, thickness, and oxygen pressure

In our previous work, we identified oxygen pressure as a critical parameter during PLD precursor deposition that controlled the eventual polymorph. High pressure-deposited precursors produced anatase, intermediate pressures produced brookite, and the lowest pressures produced rutile, although the exact pressures depended on the precursor thickness.[8] That observation remains generally true for RF sputter precursor deposition, although the boundaries of the dominant phase in pO_2/thickness space are shifted, as noted in the Results section. This shift may be related to the fact that pO_2 is also the total pressure during PLD deposition, whereas the total pressure is constant during sputtering and the partial pressure of oxygen varies. In the sputter system, it is also more difficult to obtain a wide pO_2 range, so we do not report a comparable phase diagram. Other researchers have reported on the influence of oxygen pressure in sputtered TiO_2 films. Rafieian *et al.*[14] demonstrated that oxygen deficient sputtering conditions favor rutile over anatase in a system similar system to ours, but brookite is not mentioned. In the study on the effects of oxygen interruption in RF magnetron sputtering of TiO_2 films on heated substrates, Pereira *et al.*[15] observed that during times of depleted O_2, there is a slight increase in the incidence of rutile and brookite over anatase, but they do not produce phase-pure films and their films never form the amorphous phase.

We next address the question of whether thickness itself is a determining factor in the final polymorph. In PLD, the strongly

directional evaporant plume produces films of non-uniform thickness. It must be true, then, that thinner areas of the films also correspond to slower deposition rates. We observed a correlation between the final polymorph and the thickness of the film in that system, but was thickness simply a proxy for rate? It proved more difficult than we anticipated to implement a convincing control process in the previous PLD method, but the present sputter deposition method provided large, uniform thickness films and the rate was controllable by the sputter power, although presumably the plasma energetics are also different. The pO_2 also influenced the rate to a lesser degree, so we kept the pO_2 constant at the value that was the "sweet spot" for brookite production. As Fig. 3 shows, the lower deposition rate, near 1.5 nm/min, produces precursors that anneal into anatase, regardless of thickness, whereas the higher deposition rate, near 2 nm/min, produces only brookite precursors (thinner) and rutile precursors (thicker). Thus, the deposition rate is also a key parameter in precursor preparation, separate from thickness. However, the thickness remains a second key parameter, along with the oxygen deficiency as discussed earlier. Later work on PLD-deposited precursors[16] shows that PLD-deposited precursors produced with 30 Hz pulses produce faster brookite growth fronts than the precursors produced with 10-Hz pulses. The present finding corroborates in the sputter system the similar finding in the PLD system. One sample in Fig. 3 is instructive. It is 65-nm thick and an 80:20 :: rutile:brookite mix of roughly uniform in thickness over a large centimeter-scale area. Like all of our sputter-produced precursors, the substrate is held on the platen with a clip, and the TiO_2 thickness goes to zero near the clip over a distance of about 1 mm. In the main part of the films, brookite exists as thin grains (2 μm × 10 μm) within a sea of rutile. Where the film thickness starts to decrease (and also the deposition rate of course), the sample transitions through an equal mix of similar sized grains to pure brookite. Decreasing thickness leads to the presence of anatase grains, and the thinnest section (also the most slowly deposited) is pure anatase. Thus, the correlation of polymorph formation with amorphous precursor preparation is very robust and has now been repeated in many different ways.

In the study on how TiO_2 phase and morphology are affected by pulsed-DC and RF powered magnetron co-sputtering of thin films on heated substrates, Lelis *et al.*[17] observed that anatase is formed at lower sputter power and argued that the species in the plasma are less energetic and are unable to locate the thermodynamic equilibrium phase, rutile, whereas at higher power, rutile is indeed formed. Our experiment adds new information: the amorphous precursors deposited at different rates also form rutile (or brookite) at higher power and anatase at lower power, but not *in situ* when the depositing species are energetic, but rather after annealing at a later time. This means that the precursors retain memory of the deposition conditions in some way. Either additional energy is stored, perhaps as strain,[8] to be released when the anneal procedure provides some enough additional energy to overcome the nucleation or growth barrier. Another possibility is that the sputter power affects oxygen incorporation in the growing film and once again oxygen deficiency is the primary factor.

Optical and electrical characterization

The optical characterization adds confirmation that oxygen deficient precursors produce brookite and rutile. These precursors absorb, more strongly than do anatase precursors, visible light in the range reported to be typical of oxygen vacancy absorption ($\lambda > 700$ nm).[18] The electrical measurements of the crystalline films yield to conventional activation energy analysis, suggesting conventional band transport with donor states of some tens to hundreds of meV below the conduction band, depending on the details of preparation. The oxygen-deficient amorphous precursors are also conductive, and the resistivity data fit slightly better to a hopping conductivity model. We find both resistivity increase and decrease after annealing. There is evidently a trade-off between increased mobility due to crystallinity (hence decreased resistivity) and charge carrier decrease due to oxygen vacancy filling (hence increased resistivity). We do not know how to control this yet.

SUMMARY

We produce large, fully crystalline films of a particular polymorph of TiO_2 by annealing RF sputter-deposited amorphous precursor films that are carefully prepared to control the oxygen content, the deposition rate, and the thickness. In particular, brookite, an uncommon metastable polymorph, is reproducibly obtained with uniform thickness over cm-scale area. Anatase results when the precursors are closest to stoichiometric, brookite results from slightly oxygen deficient precursors, and rutile from even more oxygen deficiency. The deposition rate and film thickness are also important factors. Anatase alone results when the rate is low, and brookite and rutile require the precursors to have been deposited faster, which presumably stores more energy in the amorphous precursor system. Finally, the thickness itself is important. If precursors are sufficiently oxygen deficient and have been deposited fast enough to form brookite or rutile, they will form brookite when they are thinner and rutile when thicker. The exact parameters that define the regions where anatase, brookite or rutile form vary slightly with the deposition method, which may have to do with the details of the deposition energetics. The end result of the annealing process seems to be defined during the deposition.

SUPPLEMENTARY MATERIAL

See the supplementary material for more details on the WAXS and EPMA analyses.

ACKNOWLEDGMENTS

This work was supported as part of the Center for Next Generation Materials by Design: Incorporating Metastability, an Energy Frontier Research Center funded by the U.S. Department of Energy, Office of Science, Basic Energy Sciences under Award No. DE-AC3608GO28308. A.P. acknowledges funding from an Oregon State University SURE Science award. We acknowledge the use of facilities at Oregon State University: MASC for sputter deposition, Professor Gregory Rorrer for the use of the Raman spectrometer, and Professor Douglas Keszler for the ellipsometer. The EPMA measurements were performed at the University of Oregon's CAMCOR facility. We are thankful to Pritha Biswas and Cameron Stewart for help with analysis.

REFERENCES

[1]J. Zhang, P. Zhou, J. Liu, and J. Yu, Phys. Chem. Chem. Phys. **16**, 20382 (2014).

[2]E. György, G. Socol, E. Axente, I. N. Mihailescu, C. Ducu, and S. Ciuca, Appl. Surf. Sci. **247**, 429 (2005).

[3]S. Yin, K. Ihara, B. Liu, Y. Wang, R. Li, and T. Sato, Phys. Scr. **T129**, 268 (2007).

[4]D.-H. Kim, W.-S. Kim, S. Kim, and S.-H. Heong, ACS Appl. Mater. Interfaces **6**, 11817 (2014).

[5]J.-G. Li, T. Ishigaki, and X. Sun, J. Phys. Chem. C **111**, 4969 (2007).

[6]A. Di Paola, M. Bellardita, and L. Palmisano, Catalysts **3**, 36 (2013).

[7]J. E. S. Haggerty, L. T. Schelhas, D. A. Kitchaev, J. S. Mangum, L. M. Garten, W. Sun, K. H. Stone, J. D. Perkins, M. F. Toney, G. Ceder, D. S. Ginley, B. P. Gorman, and J. Tate, Sci. Rep. **7**, 15232 (2017).

[8]J. S. Mangum, O. Agirseven, J. E. S. Haggerty, J. D. Perkins, L. T. Schelhas, D. A. Kitchaev, L. M. Garten, D. S. Ginley, M. F. Toney, J. Tate, and B. P. Gorman, J. Non-Cryst. Solids **505**, 109–114 (2019).

[9]X. Rocquefelte, F. Goubin, H.-J. Koo, M.-H. Whangbo, and S. Jobic, Inorg. Chem. **43**, 2246 (2004).

[10]See http://rruff.info/ for RRUFF Project database; accessed December 2019).

[11]Y. Hishikawa, N. Nakamura, S. Tsuda, S. Nakano, Y. Kishi, and Y. Kuwano, Jpn. J. Appl. Phys., Part 1 **30**, 1008 (1991).

[12]T. Sekiya, K. Ichimura, M. Igarashi, and S. Kurita, J. Phys. Chem. Solids **61**, 1237 (2000).

[13]B. Morgan and G. Watson, J. Phys. Chem. C **114**, 2321–2328 (2010).

[14]D. Rafieian, W. Ogieglo, T. Savenije, and R. G. H. Lammertink, AIP Adv. **5**, 097168 (2015).

[15]A. L. J. Pereira, P. N. Lisboa Filho, J. Acuña, I. S. Brandt, A. A. Pasa, A. R. Zanatta, J. Vilcarromero, A. Beltràn, and J. H. Dias da Silva, J. Appl. Phys. **111**, 113513 (2012).

[16]J. S. Mangum, L. M. Garten, D. S. Ginley, and B. P. Gorman, J. Am. Ceram. Soc. **00**, 1–9 (2019).

[17]M. Lelis, S. Tuckute, S. Varnagiris, M. Urbonavicius, G. Laukaitis, and K. Bockute, Surf. Coat. Technol. **377**, 124906 (2019).

[18]Y. Yang, L.-C. Yin, Y. Gong, P. Niu, J.-Q. Wang, L. Gu, X. Chen, G. Liu, L. Wang, and H.-M. Cheng, Adv. Mater. **30**, 1704479 (2018).